



Published in final edited form as:

Genes Immun. 2010 December ; 11(8): 609–621. doi:10.1038/gene.2010.39.

Genome-wide association identifies SKIV2L and MYRIP as protective factors for age-related macular degeneration

Laura J Kopplin¹, Robert P Igo Jr², Yang Wang², Theru A Sivakumaran², Stephanie A Hagstrom^{4,6}, Neal S Peachey^{4,5,6}, Peter J Francis⁷, Michael L Klein⁷, John Paul SanGiovanni⁸, Emily Y Chew⁸, Gayle JT Pauer⁴, Gwen M Sturgill⁵, Tripti Joshi², Liping Tian², Quansheng Xi², Alice K Henning⁹, Kristine E. Lee¹⁰, Ronald Klein¹⁰, Barbara EK Klein¹⁰, and Sudha K Iyengar^{1,2,3,\$}

¹Department of Genetics, Case Western Reserve University, Cleveland, Ohio, 44106, USA

²Department of Epidemiology and Biostatistics, Case Western Reserve University, Cleveland, Ohio, 44106, USA

³Department of Ophthalmology, Case Western Reserve University, Cleveland, Ohio, 44106, USA

⁴Cole Eye Institute, Cleveland Clinical Foundation, Cleveland, Ohio, 44195, USA

⁵Research Service, Veteran Affairs Medical Center, Cleveland, Ohio, 44106, USA

⁶Department of Ophthalmology, Cleveland Clinic Lerner College of Medicine of Case Western Reserve University, Cleveland, Ohio 44195 USA

⁷Casey Eye Institute, Oregon Health & Science University, Portland, Oregon, 97239, USA

⁸Division of Epidemiology and Clinical Applications, National Eye Institute, Bethesda, Maryland, 20892, USA

⁹The EMMES Corporation, Rockville, Maryland, 20850, USA

¹⁰Department of Ophthalmology and Visual Sciences, University of Wisconsin School of Medicine and Public Health, Madison, Wisconsin, 53705, USA

Abstract

Age-related macular degeneration (AMD) is the leading cause of blindness in the elderly in the developed world. We conducted a genome-wide association study in a series of families enriched for AMD and completed a meta-analysis of this new data with results from reanalysis of an existing study of a late-stage case/control cohort. We tested the top findings for replication in 1 896 cases and 1 866 controls and identified two novel genetic protective factors for AMD. In

Users may view, print, copy, download and text and data- mine the content in such documents, for the purposes of academic research, subject always to the full Conditions of use: http://www.nature.com/authors/editorial_policies/license.html#terms

^{\$}Address Correspondence to: Sudha K. Iyengar, Ph.D., Department of Epidemiology and Biostatistics, Case Western Reserve University, Wolstein Research Building Room 1315, 2103 Cornell Rd, Cleveland, OH 44106, Phone: (216) 368-5630, Fax: (216) 368-4880.

Conflict of Interest

The authors declare no conflict of interest.

Supplementary information is available at *Genes and Immunity's* website.

addition to the *CFH* ($p=2.3\times 10^{-64}$) and *ARMS2* ($p=1.2\times 10^{-60}$) loci, we observed a protective effect at rs429608, an intronic SNP in *SKIV2L* ($p=5.3\times 10^{-15}$), a gene near the *C2/BF* locus, that indicates the protective effect may be mediated by variants other than the *C2/BF* variants previously studied. Haplotype analysis at this locus identified three protective haplotypes defined by the rs429608 protective allele. We also identified a new potentially protective effect at rs2679798 in *MYRIP* ($p=2.9\times 10^{-4}$), a gene involved in retinal pigment epithelium melanosome trafficking. Interestingly, *MYRIP* was initially identified in the family-based scan and was confirmed in the case-control set. From these efforts, we report the identification of two novel protective factors for AMD and confirm the previously known associations at *CFH*, *ARMS2* and *C3*.

Keywords

macular degeneration; association testing; melanosome trafficking

Introduction

Age-related macular degeneration (AMD) is a leading cause of blindness in elderly populations worldwide. Clinically, AMD is a progressive disease, proceeding from the development of macular soft drusen and pigmentary abnormalities in early stages and culminating in vision impairing end stage forms, geographic atrophy and choroidal neovascularization.^{1–4} The etiology of AMD is multifactorial and includes modifiable risk factors such as smoking and diet in addition to genetic factors.^{5; 6} Recent efforts have strongly implicated variants in the complement cascade that modify AMD risk, with consistent evidence at the complement factor H (*CFH*), complement factor B (*BF*) / complement component 2 (*C2*) and complement component 3 (*C3*) genes.^{7–14} Variants at the age-related maculopathy susceptibility 2 (*ARMS2*) locus have been shown to increase AMD risk^{15–20} as have variants in the mitochondrial genome,^{21; 22} indicating a role for mitochondrial function in the pathogenesis of this condition.

Biological evidence also supports an immune-mediated mechanism for AMD pathogenesis. In AMD, it is believed that the ability of *CFH* to inhibit the complement cascade is impaired, resulting in inflammatory damage to surrounding tissues. Several lines of evidence support this mechanism. Immunoglobulin and complement attack complexes are present in drusen²³, indicating complement activation even at earlier stages of disease. *CFH* is found locally in the eye, being observed in choroidal capillaries, in the subRPE space, and attached to Bruch's membrane, which underlies the RPE^{9; 24; 25}. The RPE itself also appears to be a local source of *CFH*²⁴. An aged *CFH* knockout mouse model exhibits increased accumulation of lipofuscin within the RPE that is likely to predispose to impairment in RPE cell function²⁶. Despite this evidence, the question remains as to why the macula itself remains particularly susceptible to damage by the complement cascade and whether additional risk factors specific to the retina may remain to be discovered.

To identify novel loci and validate existing loci for AMD, we completed genome-wide association testing in a cohort of 161 controls and 377 cases with late AMD (Age Related

Eye Disease Study; AREDS) in conjunction with a family-based genome-wide association scan (Family Age Related Maculopathy Study; FARMS) that assessed the entire spectrum of disease severity. Examining patients with a range of endpoints enabled us to identify initiating events in disease pathogenesis in addition to confirming existing loci. The strategy of using family-based cohorts, such as the SardiNIA and Framingham subjects, as discovery cohorts both alone and in combination with traditional case-control cohorts has proven a successful means to identify variants associated with disease in the general population.^{27–30} Our discovery efforts were followed up by replication in five case-control cohorts to determine which variants are most likely to contribute to AMD (Figure 1).

Results

Genome-wide association testing was completed in the FARMS and AREDS discovery sets. Quantile-quantile plots of the observed distribution of corrected p-values versus the expected distribution (Figure 2) reveal a number of SNPs with p-values more significant than expected under the null hypothesis in the discovery cohorts. In AREDS, 51 SNPs were significant at $p = 10^{-4}$ (Table S4). Of these, 38 SNPs were located at previously identified AMD risk loci (*CFH*, *ARMS2/HTRA1*, *C2/CFB*). Within FARMS, 35 SNPs were significant at the $p = 10^{-4}$ level. Five of these SNPs were located at the *CFH* locus; the remaining 30 SNPs were located in regions not previously implicated in AMD (Table S5).

All SNPs with $p = 10^{-4}$ in either the FARMS or AREDS cohorts as well as additional variants in *CFH*, *ARMS2*, *C2/BF* and *C3* loci were advanced to replication in five Caucasian case/control cohorts. Because other complement genes do not show significant evidence in our discovery cohorts at $p = 10^{-4}$ they were not assessed in our replication set. In addition to the previously known loci, we examined novel genes that among other functions have a role in vesicular and melanosome trafficking. SNPs were genotyped using a used a 768-SNP custom Golden Gate Illumina panel in 1896 cases and 1866 controls and tested for association using logistic regression.

CFH and ARMS2

At the two best known AMD risk loci, *CFH* and *ARMS2*, we observed strong association in both the discovery and replication cohorts (Table 1, Table S8). We observed a broad signal of association across the *CFH* locus in all cohorts due to the presence of copy number polymorphisms and linkage disequilibrium (Figure S1). The extensively studied non-synonymous *CFH* Y402H variant showed evidence of association ($p = 4.0 \times 10^{-42}$); however, a number of non-coding variants were more significantly associated with AMD. The most significant non-coding variant, rs1329428, appears to exert a protective effect on AMD risk ($p = 3.2 \times 10^{-64}$). As the signal on chromosome 10q26 is distributed at two adjacent loci, *ARMS2* and *HTRA1*, we characterized association at this extended locus using dense SNP coverage in our replication set (Figure 3, Figure S2). Strong evidence for single SNP association was observed at markers in the *ARMS2* and *HTRA1* genes (Table 1), with the best evidence at the *ARMS2* A69S (rs10490924) coding variant ($p = 1.2 \times 10^{-60}$), at rs3750848, an *ARMS2* intronic SNP ($p = 8.1 \times 10^{-60}$), and at rs3793917, a *HTRA1* promoter polymorphism ($p = 4.2 \times 10^{-57}$). These three SNPs proved to be in tight disequilibrium in our

cohorts ($r^2 > 0.91$). To identify the SNPs at the *ARMS2* locus that best account for the effect this region has on AMD risk, we completed a stepwise selection analysis in our the replication set using 33 markers spanning *PLEKHA1*, *ARMS2* and into intron 3 of *HTRA1*. We found that the most parsimonious set consisted of two SNPs: rs3750848 in *ARMS2* and rs2736917 in *HTRA1* with the *ARMS2* SNP entering the model first. rs2736917 is in low LD with rs3750848 ($r^2 = 0.04$) and appears to represent an independent protective effect not previously reported.

Our best evidence for association localized to a 14-kb region including *ARMS2* and into the first intron of *HTRA1*. We identified 11 markers spanning this region and tested haplotypes for association with AMD (Figure 3, Table S6). From six haplotypes with a frequency greater than 1%, we identified one risk haplotype (OR = 2.6, $p = 1.91 \times 10^{-48}$) which contained the risk alleles at rs10490924, rs3750848 and rs3793917 (T-C-G) and four closely related protective haplotypes. The selection of rs3750848 in our stepwise selection likely represents the association due to this haplotype. Three of the core SNPs in our risk haplotype defined the earlier reported risk haplotype noted to carry an insertion/deletion polymorphism which affects RNA and protein expression of *ARMS2*.²⁰ To determine the distribution of our risk haplotype in global populations, we examined phased haplotypes from the HapMap2 populations. A higher frequency of the risk haplotype was observed in Asians (JPT/CHB) (0.41) than in CEU (0.21) or YRI populations (0.19) (Figure 4). The risk haplotype has a frequency between that of Caucasians and Asians in individuals of Indian descent, the Gujarati Indians in Houston (GIH) (0.33), indicating this population shares genetic risk factors for AMD with Asian populations. We have demonstrated that the Asian genome has very few *CFH* risk haplotypes (T.A.S., unpublished data). Our results concur with findings described by DeWan *et al*¹⁵ that the *ARMS2* region is likely the major genetic risk factor for AMD within Asian populations.

C2/BF and SKIV2L

Other strong effects for AMD have been reported at *C2/BF* and *C3*, factors that act as activators of *C3* convertase in the classical and alternative complement pathways respectively. Similar to other studies, we observed a protective effect associated with the R32Q *BF* variant^{11; 13; 31} ($p = 6.8 \times 10^{-14}$), but also found strong signals at other marker loci (Table 1, Table S8, Figure 5). rs429608, an intronic SNP in *SKIV2L*, a gene close to *BF*, displayed the best evidence for association at this locus ($p = 5.3 \times 10^{-15}$). rs438999 in *RDBP*, a gene adjacent to *BF*, ($p = 1.8 \times 10^{-13}$) and rs550605 in *C2* ($p = 2.1 \times 10^{-13}$) were also significant. Because R32Q was imputed in our data set, we verified the accuracy of imputation based on the HapMap CEU cohort, and found that our imputation was indeed highly accurate (88.2% concordance). Within the replication cohorts, rs429608 displayed only moderate disequilibrium with the R32Q variant (r^2 ranging from 0.46 to 0.61) making it less likely rs429608 is merely acting as a proxy for the *BF* variant (Figure S5). rs550605 and rs438999 were in high LD both with each other and with R32Q ($r^2 = 0.85$). The high LD of these SNPs with R32Q provides additional confidence in the accuracy of the R32Q imputation since the results of association testing for these three SNPs was similar in magnitude. To determine whether these effects were independent from the effects of the *CFH* and *ARMS2* loci on AMD, in our replication cohorts we adjusted for principal

components that account for the majority of the SNP variation at *CFH* and *ARMS2*. Strong signals of association remained at R32Q ($p = 1.8 \times 10^{-10}$), rs429608 ($p = 5.2 \times 10^{-10}$), rs550605 ($p = 4.1 \times 10^{-10}$) and rs438999 ($p = 1.3 \times 10^{-9}$). These findings provide evidence that the protective effect at this region is separate from the effects observed at *CFH* and *ARMS2*, and that variants other than the *BF* R32Q variant may contribute to this effect.

To dissect the signal further we took the three most significant chromosome 6 findings and sequentially conditioned on the minor allele of each variant. None of the variants entirely accounted for the effect at this locus. The conditional results from rs641153 in *BF* and rs550605 in *C2* were quite similar, as is expected given the high LD between these markers. Conditioning on either rs429608 in *SKIV2L* or rs641153 did not entirely eliminate the signal at the other SNP (Table S7). Haplotype analysis of 13 SNPs spanning from *C2* to *SKIV2L* identified 5 common (frequency > 1%) haplotypes. We identified one highly protective haplotype, which harbored the C-A-G-A alleles at rs550605, rs641153, rs438999 and rs429608 (OR = 0.43, 95% CI = [0.32, 0.56]; $p = 1.2 \times 10^{-9}$) and another closely related protective haplotype (Figure 5, Table S6). One single risk haplotype was observed (OR = 1.36, 95% CI = [1.18, 1.57]; $p = 1.9 \times 10^{-5}$). Additionally, we identified a secondary protective haplotype (OR = 0.72, 95% CI = [0.55, 0.93]; $p = 0.01$) that was identical to our risk haplotype with the exception of the protective allele of rs429608. Thus, a haplotype harboring the risk allele of the *BF* R32Q polymorphism and the protective allele of *SKIV2L* rs429608 was found to be protective. Of the two genotyped SNPs in *C3*, R102G also shows strong association in this study but was not pursued by further fine-scale mapping ($p = 1.40 \times 10^{-8}$).

MYRIP

The strongest novel signal in our meta-analysis came from the family-based GWAS (Table 1, Table S8). We identified a novel protective effect at *MYRIP*, a protein that enables the trafficking of melanosomes in the RPE.^{32; 33} The best initial signal was observed in the FARMS cohort at rs11129874 ($p = 8.31 \times 10^{-5}$). rs2679798, another variant in *MYRIP*, displayed the best evidence of association in meta-analysis ($p = 2.9 \times 10^{-4}$). The rationale for the difference is that the family-based association may identify more highly penetrant rare variants. We identified a risk and protective haplotype using the three *MYRIP* SNPs included in replication. The haplotypes showed evidence for association similar to the individual SNPs indicating the three SNPs are capturing the same signal, likely due to high LD between them ($r^2 > 0.7$). The protective effect at *MYRIP* is independent of the effects of *CFH* and *ARMS2* on AMD as the association remained following adjustment for *CFH* and *ARMS2* variations using principal components (rs2679798, $p = 0.001$). Given its biological function, *MYRIP* remains an interesting new candidate, despite not reaching genome-wide significance.

UNC13C

In FARMS, *UNC13C*, a protein that regulates synaptic vesicle fusion,^{34; 35} showed strong evidence for association (rs885203, $p = 2.2 \times 10^{-5}$). Variants in this gene did not show association within the population-based replication cohorts; however, *UNC13C* localizes to the 15q linkage region previously identified in the FARMS cohort³⁶. Two other *UNC13C*

variants, rs10444833 and rs11635375, were also associated with AMD ($p=9.6\times 10^{-4}$, $r^2=1$) and these variants account for a significant portion of the linkage signal mapping to this region (Figure S4).

Discussion

Genetic studies have identified strong effects in complement pathway genes and *ARMS2/HTRA1* on AMD. However, identification of major genes such as *CFH* and *ARMS2* has not revealed why the macula, a region rich in cone photoreceptors, seems to be especially vulnerable to the AMD disease process. *ARMS2*, localizing to mitochondria-dense retinal photoreceptors, has a potential role in events that may contribute to disease progression. In particular, mitochondrial respiratory proteins of photoreceptors may accumulate photo-oxidative defects in these post-mitotic cells. Many potential functions have been ascribed to *CFH*, but an underappreciated and recent discovery is that *CFH* has a role in proper distribution of melanosomes.²⁶ *CFH* deficiency in aged knockout mice shows that there are changes in the distribution of melanosomes, melanosome-lipofuscin and lipofuscin particles, which are associated with retinal abnormalities and visual dysfunction. Ocular melanin has antioxidant properties and proper distribution of the melanosomes in the retinal pigment epithelium (RPE) cells ameliorates photooxidative damage.

Two genes linked to AMD in this paper, *CFH* and *MYRIP*, are now seen to share a significant role in melanosome trafficking or biogenesis, among other mechanisms.^{26; 32; 33} Inappropriate trafficking of melanosomes impairs phagocytic and autophagic degradative processes in RPE cells, including the phagocytosis of photoreceptor outer segments, which is accomplished exclusively by the RPE and is critical for maintaining outer retinal integrity. RPE cells also protect the retina from reactive oxygen species that are generated in response to light exposure³⁷. A primary effect of RPE exposure to oxidative species is the generation of non-degradable byproducts such as lipofuscin, which contribute to the decline of RPE function with aging^{38; 39} *MYRIP* may contribute to these protective effects by minimizing RPE reactive oxygen species exposure and, subsequently, the accumulation of lysosomal impairing oxidized complexes, preventing or delaying declines in RPE function. In this regard, it is interesting to note that progressive stages of AMD, particularly in the dry form, involve either retinal hyperpigmentation, or depigmentation. Guo et al⁴⁰ concluded that the absence of melanin increases RPE light absorption by ~20%. These observations together with our results suggest that melanosome trafficking may be under-appreciated as an important contributor to AMD, connecting essential functions of known genes, e.g. *CFH*, to a specific pathway within these specialized and polarized cells.

Novel protective factors

Prior work on retinal degenerations has demonstrated that specialization of the RPE/choroid for color vision and visual acuity renders key effectors susceptible to genetic abnormalities. Mutations in myosin VIIA, an unconventional myosin strongly expressed in the RPE and photoreceptor outer segments, result in Usher syndrome type IB (MIM 276900), characterized by progressive retinitis pigmentosa with onset in the first decade of life.^{41–44} Interestingly, myosin VIIA interacts with *MYRIP* to traffic melanosomes to the apical

processes of RPE cells.^{33; 45; 46} Thus, the melanosome trafficking pathway shares genetic links with early onset degenerative retinal disease as well as AMD. It is possible that weak alleles for Mendelian retinal degenerations may predispose to later onset retinal disease such as AMD. In the FARMS discovery cohort, the *MYRIP* association signal localizes to the 3' end of *MYRIP* and the adjacent downstream region. The 3' end of the *MYRIP* gene codes for a Myrip-Mlph conserved amphipathic helix domain and a *MYRIP* specific domain required to mediate interactions with myosin VIIA.⁴⁷

RPE dysfunction occurs early in AMD pathogenesis and we propose that changes in melanosome localization within the RPE are an initiating factor for early stage disease. *MYRIP* was originally identified in the FARMS cohort, a family-set capturing the spectrum of AMD severity, including early pathogenic changes. Replication efforts support a protective effect of *MYRIP* variants, although a genome-wide significance threshold was not met. This may be due in part to the magnitude of the protective effect and the late-stage disease phenotype used to define the replication cases. Each protective allele at rs2679798 reduces the risk of AMD 0.86-fold or by approximately one step on the 15-step AMD severity scale. Further study of *MYRIP* in larger cohorts and groups with early AMD cases will be necessary to further define the contribution of this gene to AMD pathogenesis. Nonetheless, *MYRIP*'s role in the appropriate localization of melanosomes to RPE apical processes makes it a plausible biological candidate for mediating early stage AMD.

Inappropriate trafficking of melanosomes impairs phagocytic and autophagic degradative processes in RPE cells, including the phagocytosis of photoreceptor outer segments, a key support role in maintaining retinal health.^{48–51} RPE cells are believed to protect the retina from the generation of reactive oxygen species in response to light exposure³⁷. A primary effect of RPE exposure to oxidative species is the generation of non-degradable byproducts such as lipofuscin, which contribute to the decline of RPE function with aging^{38; 39}. A possible mechanism by which *MYRIP* exerts a protective effect is by minimizing RPE reactive oxygen species exposure and, subsequently, the accumulation of lysosomal impairing oxidized complexes, preventing or delaying declines in RPE function.

SKIV2L shares homology with two yeast exosome components, *Mtr4p* and *Ski2p*.^{52; 53} Based on studies of the yeast counterparts, it is thought that *SKIV2L* acts as an RNA helicase with a role in exosome recruitment or activation.^{53; 54} McKay et al¹² earlier reported a coding SNP, R151Q, in *SKIV2L* as showing a significant protective effect for AMD ($p=0.0004$), but could not ascertain if this effect was independent of *BF* R32Q with which it shares extensive LD ($r^2 .95$). Our results indicate there may be a second independent effect at this locus and point to another SNP in *SKIV2L*, rs429608, or a SNP in very high LD, as the mediator of this effect. Initial studies of this region focused exclusively on *C2* and *BF* due to their roles in the complement pathway^{11; 13; 31} and did not extend their investigations to neighboring genes such as *SKIV2L*. Future investigations should include variation beyond that found in the *C2* and *BF* genes, as we have demonstrated non-*C2/BF* variants that may contribute to this region's protective effect.

SKIV2L is involved in the degradation of RNAs by the exosome and may have a role in autophagy.^{55; 56} Increased RPE autophagy has recently been linked to drusen formation

and autophagic markers are present in drusen.⁵⁷ As rs429608 is an intronic variant it does not directly alter the structure of *SKIV2L*. Non-coding variants may still affect patterns of gene expression through the disruption of regulatory elements controlling gene transcription or splicing and translation. The minor allele of rs429608 is predicted to disrupt a transcription factor binding site for early B-cell factor, a transcription factor involved in early B-lymphocyte development. A 3'UTR variant in *SKIV2L* has recently been reported to exert a protective effect in polypoidal choroidal vasculopathy, a hemorrhagic macular disease that shares some features with neovascular AMD,⁵⁸ delineating a possible role for *SKIV2L* in protection from neovascular events. *SKIV2L* is highly expressed in T and B lymphocytes and dendritic cells, and variants in *SKIV2L* have also been associated with increased risk for systemic lupus erythematosus (SLE), an autoimmune disorder in which the immune system attacks the body's own organs causing inflammatory damage.⁵⁹ *SKIV2L* may exert its protective effect through modulating the immune response.

Loci implicated in the AREDS discovery cohort were not replicated beyond the regions of known association at *CFH*, *ARMS2*, chromosome 6 and C3, similar to findings from two previous studies⁶⁰; ⁶¹. Our re-analysis of the AREDS GWAS data identified 67 SNPs significant at $p = 10^{-4}$ prior to genomic control correction, 24 of which were at potentially novel loci. This represents a reduction in the number of novel SNPs significant at this threshold from the initial AREDS dbGaP data (58 novel SNPs)⁶⁰. The exclusion of non-Caucasian subjects and the inclusion of age into the regression models in our analysis may account for this difference. Four SNPs at novel loci demonstrated a trend towards association in the Edwards *et al* replication cohort⁶⁰. One of these SNPs, rs8056814, was also tested in our replication efforts and did not display evidence for association ($p=0.10$). We did not test the other 3 SNPs since they did not meet the $p = 10^{-4}$ threshold in our AREDS GWAS re-analysis. Similarly, rs9288410, the only novel SNP displaying association in the replication efforts of Zhang *et al*,⁶¹ did not meet our inclusion threshold and was not examined further.

CFH and ARMS2 Loci

Diverse populations have been examined for *CFH* and *ARMS2* associations^{62–66} and it is evident that risk variants at these loci may not underlie disease to the same extent in populations of different ancestry. We observed that the frequency of the *ARMS2* risk haplotype in the HapMap CEU, YRI, JPT and CHB and HapMap3 populations varied substantially. The *ARMS2* risk haplotype is observed at a higher frequency in Asian populations than is seen in Caucasian and African counterparts. This finding corroborates the genomewide association results of Dewan *et al.*, who observed association at the *ARMS2/HTRA1* region, but not *CFH* in a cohort of Southeast Asians from Hong Kong.¹⁵ Recent observations indicate that the majority of Asians do not carry risk haplotypes at the *CFH* locus, while *CFH* risk haplotypes are common in Caucasians (T.A.S., unpublished data). It is not known whether these differences in genetic risk at *CFH* and *ARMS2* may account for differences in the frequency and type (neovascular vs geographic atrophy) of late AMD profiles in Asians and Caucasians. Asians exhibit a predisposition for the development of exudative disease rather than geographic atrophy,⁶²; ^{64–66} implying

perhaps *ARMS2* variants may encourage progression to neovascular end stage disease whereas *CFH* variants promote geographic atrophy.

The core *ARMS2* risk haplotype we identified corresponds to a haplotype reported to harbor an insertion/deletion polymorphism that affects *ARMS2* expression. The initial report of the *ARMS2* indel polymorphism found this variant to be in complete linkage disequilibrium with the *ARMS2* risk haplotype ($r^2=1$). However, further studies have identified individuals with the A69S risk allele that do not harbor the indel^{67; 68}. We genotyped the indel using PCR in 161 samples from several ethnic groups including individuals from the HapMap JPT and CHB populations and Caucasian and African American subjects from the Coriell Human Diversity Panels (Figure S3). Our results indicate that the reported *ARMS2* indel polymorphism resides on our identified risk haplotype. Our stepwise selection identified two SNPs, rs3750848 and rs2736917, which account for the effect at this locus. rs3750848 is an intronic variant in *ARMS2* that resides in an LD block with the well characterized *ARMS2* rs10490924 variant and with rs3793917, an *HTRA1* promoter polymorphism, both of which were also highly associated with AMD in our cohorts. rs3750848 probably serves as a surrogate for our risk haplotype in the stepwise selection model and likely represents the effect of the indel. rs2736917 is an intronic SNP in *HTRA1* that seems to exert an independent protective effect. This supports the recent findings by Yang *et al.* that the AMD risk haplotype at this locus affects expression of both *ARMS2* and *HTRA1* and that variation in both genes may mediate AMD susceptibility⁶⁹.

In 1 896 affected cases, 11% did not have risk haplotypes at either the *CFH* or *ARMS2* loci. Of these subjects, 96% had at least one risk haplotype at the *SKIV2L* locus, each copy of which increases the odds of AMD 1.30-fold. In the absence of the major *CFH* and *ARMS2* risk factors, perhaps rare variants, with mild functional impacts on trafficking pathways may also contribute to disease in these subjects. Initial evidence for such a hypothesis is observed in our familial cohort at the *UNC13C* locus. Variants at this region account for a portion of the linkage signal localized to 15q in a prior study of the FARMS cohort³⁶. *UNC13C* regulates synaptic vesicle fusion, a process that uses much of the same trafficking machinery as lysosomal derived organelles, like melanosomes, to deliver vesicles to the synapse.^{70; 71} While *UNC13C* did not show evidence for association in our case/control cohorts, rare variants may predispose to AMD in a subset of patients and require deep resequencing to identify.

In summary, our findings demonstrate that *SKIV2L* variants may underlie the protective effect at the AMD chromosome 6 locus and confirm known associations at *CFH*, *ARMS2* and *C3*. These results further establish the link between inflammatory and oxidative stress pathways and AMD. The discovery of a protective effect associated with *MYRIP* highlights melanosome trafficking as an underexplored pathway for AMD pathogenesis. Within the retina, melanosome trafficking occurs exclusively in the RPE. *MYRIP* thus represents the first RPE specific AMD genetic modifier to be identified and provides insight into how RPE dysfunction may initiate AMD.

Methods

Genome-wide Association Study (GWAS) subjects

Family Age Related Maculopathy Study—The FARMS cohort included 293 individuals aged 26–90 years from 34 extended families, recruited through severely affected probands at the University of Wisconsin-Madison Retina Clinic. Subjects were evaluated for AMD using a standardized clinical exam and fundus photography. Thirty-degree stereo color fundus photographs from each eye were graded as previously described³⁶ using the Wisconsin Age-Related Maculopathy Severity (WARMS) scale, a fifteen step semi-quantitative measure of AMD features based on presence and severity of characteristic lesions varying from no to late stage AMD. To create a single metric for use in association testing, values were averaged across eyes for each individual and adjusted for the effects of age and age² using regression to account for the effect of age on AMD severity. The score for each subject was adjusted to a standardized age of 80 years and transformed using a Box-Cox transformation (with power transformation parameter $\lambda = .80$) as previously described.³⁶

Age Related Eye Disease Study—The AREDS cohort included 391 late-stage cases and 188 controls aged 63–90 years collected as part of the larger AREDS clinical trial and genotyped at the Center for Inherited Disease Research. Genotype and phenotype data for this cohort is publicly available through the database of Genotype and Phenotype (dbGaP).⁷² Subjects were evaluated using a standardized clinical exam and fundus photography according to specific protocols similar to those used in the FARMS. Fundus photographs were used to assign subjects to severity categories based on the presence of drusen, pigmentary abnormalities or late stage disease.^{72–74} For the AREDS study, cases and controls were selected to represent the extremes of disease, with cases having choroidal neovascularization, geographic atrophy, or both in at least one eye and controls being free from any signs of AMD and having at most small hard drusen. The initial AREDS data set released to dbGaP included several Black and Asian subjects in addition to those reported to be of white, non-Hispanic origin. For our current analysis, we limited our study population to subjects of white, non-Hispanic origin to avoid potential effects of population stratification. We obtained permission from the AREDS operations committee to use these data in our analyses.

Replication cohorts

Age Related Eye Disease Study-Replication—AREDS-Replication (AREDS-R) consists of additional subjects from the AREDS clinical trial not already included in the discovery cohort. These subjects include 471 cases and 98 controls identified at the AREDS Reading Center using the same phenotype definition and process as in the AREDS discovery group. Cases were defined as subjects having large drusen, choroidal neovascularization, geographic atrophy, or a combination of these in at least one eye and controls were subjects free from any signs of AMD and having at most small hard drusen.

Beaver Dam Eye Study—The Beaver Dam Eye Study (BDES) is a longitudinal population-based study initiated in 1988 with 5, 10 and 15 year follow-up examinations.^{1; 2;}

75; 76 Subjects aged 43–86 years at baseline were examined at each study visit in the same fashion as the FARMS cohort and characterized for AMD using the WARMS scale. A subset of unrelated individuals from this cohort, 248 cases and 1025 controls, was included in the present study. Cases were defined as individuals with a WARMS score greater than or equal to 11 in either eye at the baseline or follow-up visits, corresponding to extensive large drusen with pigmentary changes, geographic atrophy or choroidal neovascularization. Controls were selected to have been seen at all four exam periods and to have not scored greater than a WARMS score of 4 in either eye at any time point, thus showing no signs of AMD. In the case of related subjects, only one subject was chosen for inclusion from each family, with preferential selection of cases. All subjects were of Northern European descent.

Cleveland Clinic Foundation—The Cleveland Clinic Foundation (CCF) cohort consists of sporadic cases and controls enrolled through the Cole Eye Institute at CCF. Subjects aged 51–96 years were evaluated using dilated clinical exam and assigned an AMD score based on the AREDS classification system at the time of exam. The present study includes 650 cases, with large or extensive intermediate drusen, choroidal neovascularization or geographic atrophy in at least one eye and 285 controls with at most small, hard drusen, no signs of AMD and no family history of retinal disease. Subjects were of white, non-Hispanic origin.

Oregon Health Sciences University—The Oregon Health Sciences University (OHSU) cohort was recruited as sporadic cases and controls seen at the Casey Eye Institute or as subjects enrolled as part of the Complications of Age-Related Macular Degeneration Prevention Trial. Subjects aged 57–99 years underwent dilated clinical exam by an ophthalmologist and fundus photography, and were classified according to phenotype using AREDS classifications. Cases were defined as having choroidal neovascularization or geographic atrophy in at least one eye and controls as having no signs of AMD (no drusen greater than 63 μm in diameter), with 407 cases and 219 controls included in this study. All subjects were of Northern European descent.

Veterans Affairs Medical Center—The Veterans Affairs Medical Center (VAMC) cohort, aged 60–96 years, was enrolled at the Cleveland VAMC Eye Clinic and evaluated similarly to the CCF cohort. Phenotype classification based on the AREDS classification system was assigned at the time of clinical exam. One hundred twenty cases with large or extensive intermediate drusen, choroidal neovascularization or geographic atrophy in at least one eye and 239 controls with at most small, hard drusen, no signs of AMD and no family history of retinal disease were selected for use in this study from a larger group of subjects. Chosen subjects were of white, non-Hispanic origin. Subjects with extensive small drusen, non-extensive intermediate drusen or of other ethnicities were excluded from this study.

Demographic data and AMD phenotype subtypes are included in Tables S1 and S2.

This study was approved by the Institutional Review Boards at the respective institutions. Appropriate informed consent was obtained from subjects at all participating institutions.

Genotyping and Quality Control

Family Age Related Maculopathy Study—The FARMS cohort was genotyped using the Affymetrix SNP 5.0 GeneChip at the Gene Expression and Genotyping Core Facility at Case Western Reserve University. Samples were plated by family, irrespective of case/control status, with a quality control sample included on each plate. Genotype calls were made using the BRLMM-P algorithm (Affymetrix). All samples were observed to have a sample call rate greater than 95%. Any SNPs with a call rate less than 85% or a minor allele frequency less than 5% (FREQ, S.A.G.E. v5.477) were excluded from analysis (Table S3). MARKERINFO (S.A.G.E. v5.4) was used to detect any inconsistencies in Mendelian inheritance. Apparent inheritance errors were resolved by setting to missing the genotypes of any individuals in a pedigree contributing to the error. In total, 182,503 (0.66%) individual genotypes were set to missing. After applying these quality metrics, 361,556 SNPs were tested for association. The *C3* R102G variant was genotyped using a custom Taqman assay.

Age Related Eye Disease Study—The AREDS cohort genotyping was completed by the Center for Inherited Disease Research (CIDR) and genotyping data was obtained through dbGaP.⁷² Briefly, samples were genotyped on two platforms, the Affymetrix GeneChip Human Mapping 100K Set and the Illumina Sentrix Human-1 BeadChip, although some samples were not available on the Affymetrix platform due to genotyping failure at CIDR. Genotype calls were made by the AREDS research group using BeadStudio and the BRLMM algorithm implemented in Affymetrix Power Tools v1.4.0. Samples genotyped with the Illumina platform were excluded if the median GenCall score was < 0.6 or if the sample call rate was less than 90%. For the Affymetrix platform, samples were excluded if the combined call rate across the *Hind III* and *Xba I* chips was less than 97.5%, the call rate for an individual chip was less than 94.5%, or if both chips were not completed for a sample. SNPs on either platform were excluded if they had a call rate less than 90% or a minor allele frequency less than 5%. SNPs from the BeadChip were also excluded if the SNP GenCall score was less than 0.5 (Table S3). After quality metrics were applied, 186,807 SNPs were advanced to analysis; 4,433 analyzed SNPs overlapped between the two chips. For overlapping SNPs, genotypes from the platform with the higher call rate at the given SNP were used for analysis.

Replication Panel—Replication panel genotyping was completed with an Illumina Custom Golden Gate Assay at the Genotyping Core Facility at Case Western Reserve University. All SNPs significant at the $p < 0.0001$ level in either the FARMS or AREDS GWAS analyses and additional tag SNPs at each locus selected using Tagger (pairwise tagging, $r^2 \geq 0.7$) were included in the panel. Imputation⁷⁸ was used in the AREDS discovery cohort to obtain additional data at three loci showing evidence of association in both the AREDS and FARMS cohorts and results were combined at SNPs in common using Fisher's method for combining p-values. Fisher's method was chosen for combined analysis as a phenotype represented with continuous values was tested in the FARMS cohort (as opposed to a binary trait in AREDS). The most significant combined SNPs and tag SNPs ($r^2 = 0.8$) covering these regions were included in the replication panel. Finally, markers from the known AMD susceptibility loci *CFH*, *ARMS2*, *BF/C2* and *C3* were genotyped.

Cases and controls from all cohorts were randomly assigned to plates for genotyping along with a random blind replicate and a standard HapMap sample to assess genotyping reliability. Genotype calls were made using the genotyping module in BeadStudio v3.2. Samples with call rates less than 90% or median GenCall scores < 0.6 (115 total excluded samples) were excluded from association analysis. SNPs with call rates $< 85\%$ or deviation from Hardy-Weinberg proportions ($p < 0.0001$) were also removed from further consideration (Table S3). Cluster graphs for each SNP were manually inspected and any SNPs displaying poor genotype clustering were removed. Replication panel samples were genotyped using custom Taqman assays to determine the gender of each sample for use as a quality control metric. rs1061170, the Y402H variant of *CFH*, failed design metrics for the custom Illumina panel and was genotyped using a custom Taqman assay. Three MYRIP SNPs, rs2679798, rs11129874 and rs1344189, were directly genotyped as part of this custom panel. rs641153, the R32Q *BF* variant, was unable to be genotyped as part of the Illumina panel and was subsequently imputed using MaCH (see Methods, Imputation subsection).

Statistical Analysis

Family Age Related Maculopathy Study—Family-based association testing was completed using ASSOC (S.A.G.E. v5.4). ASSOC fits a linear mixed model in which genotype for a given SNP is included as a fixed effect on the phenotype. Within-family correlations are modeled as random effects. The transformed and adjusted AMD severity scale score was tested for association with each SNP individually using an additive model that included a random sibling effect. The genomic control method⁷⁹ was applied to identify and correct for any inflation of the test statistic due to overdispersion; the inflation factor, λ , was estimated as 1.09 in the FARMS cohort. All results represent these corrected p-values.

Age Related Eye Disease Study—The multi-dimensional scaling approach implemented in PLINK⁸⁰; 81 was used to test for population stratification in the AREDS discovery cohort. Fourteen individuals were self-identified as non-Caucasian (12 Black, 2 Asian) according to phenotype records and were removed from all subsequent analyses. In total, data from 513 subjects were available from the Affymetrix 100K chip; data from 579 subjects were available from the Illumina 100K chip.

Logistic regression was used to test each SNP individually for association with the binary case/control phenotype using PLINK. Age was included in models, given the strong correlation between age and the development of AMD. For the AREDS cohort, the inflation factor, λ , was estimated as 1.04. All reported p-values were corrected for λ .

Replication Panel—Association analysis was conducted using logistic regression in PLINK in the AREDS-R, BDES, CCF, OHSU and VAMC cohorts. Within each cohort, SNPs from the custom Golden Gate assay were individually tested for association with case/control status using logistic regression models including age and sex. To combine findings across the replication cohorts, a combined effect estimate was calculated by taking the weighted average of the individual cohort effect estimates, using inverse variance as the weighting factor. This combined estimate was used to determine an overall odds ratio for

each SNP. Cohorts were analyzed separately and combined using meta-analysis to avoid introducing stratification as cases and controls were identified at different sites over differing time frames. We chose this approach because we found it to be more conservative than a combined analysis grouping all cases and controls. We also calculated Cochran's Q statistic for each SNP to test the hypothesis of homogeneity of effect sizes amongst the replication cohorts. The Q statistic is a weighted sum of the squared differences of the individual study effect sizes and the combined effect estimate. Inverse variance was used to weight each study. Results from association testing are displayed for regions reaching genome-wide significance (*ARMS2*, *SKIV2L*, *CFH*) and having dense SNP coverage (Figures 3, 5, S1, S2). *MYRIP* results are included in Table 1, but are not shown graphically due to genotyping of only three SNPs in the replication groups.

Meta-analysis—To incorporate findings from both discovery and the replication cohorts, results from the FARMS, AREDS and replication cohorts were combined using Fisher's method for combining p-values. The \log_e (p-value) of each individual cohort was calculated, summed and then multiplied by -2 to obtain a test statistic which was then compared to a χ^2 distribution with 14 df to obtain a combined p-value. In all cases, discovery p-values were corrected using genomic control prior to being included in the meta-analysis. These meta-analysis p-values are reported for all findings unless otherwise indicated.

Imputation

Imputation was completed in the FARMS and AREDS discovery cohorts and the replication cohorts using MACH1.082 and phased CEU data. MACH infers the genotypes of markers not directly genotyped within a study population by using neighboring genotyped SNPs and underlying LD patterns in the study and reference populations. SNPs with imputation R_{sq} scores less than 0.30 were excluded. The remaining SNPs were tested for association with the power transformed AMD score using ASSOC (S.A.G.E.) in the FARMS cohort or for association with case/control status via logistic regression in PLINK in the AREDS and replication cohorts. Twenty SNPs across the *BF/SKIV2L* region were used to impute 44 additional variants at the locus, including rs641153. To assess the quality of imputation at the *BF/SKIV2L* locus, we conducted a bootstrap analysis of the HapMap CEU data. In each replicate, the genotypes of ten randomly selected HapMap population individuals were masked and imputed, using the other 50 individuals as the reference sample, including only the SNPs genotyped at this region in the replication cohorts. The imputed alleles were compared with the true genotypes to determine concordance. Concordances over 1 000 independent random test samples were averaged to provide an estimate of the accuracy of imputation.

Haplotype Analysis

Haplotypes across the *ARMS2*, *MYRIP* and chromosome 6 regions were determined using PHASE v.2.1, which uses Bayesian haplotype reconstruction to assign the most likely haplotypes to each subject.^{83; 84} A subset of SNPs from the replication panel was chosen at each location for haplotyping based on inspection of the association testing results and LD across the region. At *ARMS2*, the three most significant association signals within the replication cohorts fell into a single LD block. Eleven SNPs spanning this LD block,

including these three, were used in haplotyping. Six haplotypes with frequencies greater than 1% were identified. All three successfully genotyped *MYRIP* markers were haplotyped; 4 haplotypes with frequencies greater than 1% were identified. Thirteen SNPs from *C2* to *SKIV2L* were used to create haplotypes across this locus; 5 haplotypes with frequencies greater than 1% were identified. Haplotypes were tested individually for association with case-control status within each cohort using logistic regression. Age and gender were included in all analyses.

Haplotyping at the *ARMS2* and chromosome 6 regions was also completed using the haplo.glm function in HaploStats, 85 This program performs weighted logistic regression, using the posterior probabilities of possible diplotypes as the weights, thus allowing for uncertainties in haplotype phasing to be accounted for in association testing. The most common haplotype at each region was chosen as the baseline haplotype to which other haplotypes were compared. Results from this analysis were similar to our findings using the most likely haplotype for each subject and are presented in Supplemental Table S6.

Adjusting for Effects of *CFH* and *ARMS2*

To test *SKIV2L* and *MYRIP* AMD relationships in the context of risk associated with numerous *CFH* and *ARMS2* variants we first applied principal components analysis to identify eigenvectors accounting for the majority (80%) of the SNP variation at the *CFH* and *ARMS2* regions. A principal components analysis approach was chosen due to the complex nature of risk modifiers at the *CFH* region which contains effects of both SNP markers and copy number variants. This method allows us to capture variation due to both types of polymorphisms without having to explicitly select individual variants for inclusion in the model. The method also does not require us to declare a specific variant as causal, but merely finds the combination that is most representative of the full spectrum of variation. After adjusting for age and sex, principal component scores were sequentially added to the logistic regression model to find components with the most significant effect on AMD. At the *CFH* locus, six significant components were identified while four were selected at the *ARMS2* region. Component scores from these variables were included in the logistic regression models testing for association at *SKIV2L* and *MYRIP*.

Chromosome 6 Locus Conditional Analysis

Conditional analyses at the chromosome 6 region were completed at rs429608 at *SKIV2L*, rs641153 (R32Q) at *BF*, rs497239 at *C2* in the replication cohorts. In PLINK, the allelic dosage of each SNP was individually included as an additional covariate in the logistic regression model along with age and sex. Results were combined across the replication cohorts as described for single SNP association testing.

ARMS2 insertion/deletion genotyping

PCR primers were designed specific to sequences flanking the *ARMS2* *372_815del443ins54 insertion/deletion (indel) polymorphism (Forward primer 'CAGGACTCTCTCCACCTG', Reverse primer 'AATGCTCAGGGGCTCCTATT') to result in PCR products of different lengths dependent on the presence of the indel polymorphism. Two HapMap samples with ancestry from northern and western Europe

(CEU), NA11839 and NA12716, were used as controls for PCR genotyping with their corresponding indel genotypes, no copies and one copy, confirmed using Sanger sequencing (data not shown). Forty-nine Caucasian and 48 African American samples from the Coriell Human Diversity Panel and 27 Japanese in Tokyo (JPT) and 37 Han Chinese in Beijing (CHB) HapMap subjects were successfully genotyped for the indel polymorphism. Phased haplotypes at the *ARMS2* locus were downloaded from HapMap for the JPT and CHB subjects and Affymetrix 6.0 data was imputed and phased for the Caucasian and African American cohorts as described above using MACH1.0 and PHASE.

Supplementary Material

Refer to Web version on PubMed Central for supplementary material.

Acknowledgments

This study was supported by NIH grants EY015810, U10EY06594, EY015286, EY13438 and EY10605 from the National Eye Institute, training grant T32 EY07157 to the Visual Sciences Training Program and T32 GM07250 to the Case Medical Scientist Training Program; U.S. Public Health Service research grants GM28356, from the National Institute of General Medical Sciences; and by Senior Scientific Investigator Awards from Research to Prevent Blindness (Drs. R. Klein, B. Klein) and unrestricted awards from Research to Prevent Blindness (Departments of Ophthalmology, Case Western Reserve University (CWRU) School of Medicine and Cleveland Clinic Lerner College of Medicine of CWRU), a VA Merit Review and a Center Grant from Foundation Fighting Blindness. This research was also supported by the Gene Expression and Genotyping Facility of the Comprehensive Cancer Center at CWRU and University Hospitals of Cleveland (P30CA43703) and the Genotyping Core Facility at CWRU. The results of this paper were obtained by using the software package S.A.G.E., which is supported by a U.S. Public Health Service Resource Grant (RR03655) from the National Center for Research Resources. This publication was made possible by the CWRU/Cleveland Clinic CTSA Grant Number UL1 RR024989 from the National Center for Research Resources (NCRR), a component of the National Institutes of Health and NIH roadmap for Medical Research. Its contents are solely the responsibility of the authors and do not necessarily represent the official view of NCRR or NIH.

References

1. Klein R, Klein BE, Knudtson MD, Meuer SM, Swift M, Gangnon RE. Fifteen-year cumulative incidence of age-related macular degeneration: the Beaver Dam Eye Study. *Ophthalmology*. 2007; 114(2):253–262. [PubMed: 17270675]
2. Klein R, Klein BE, Tomany SC, Meuer SM, Huang GH. Ten-year incidence and progression of age-related maculopathy: The Beaver Dam eye study. *Ophthalmology*. 2002; 109(10):1767–1779. [PubMed: 12359593]
3. Mitchell P, Wang JJ, Foran S, Smith W. Five-year incidence of age-related maculopathy lesions: the Blue Mountains Eye Study. *Ophthalmology*. 2002; 109(6):1092–1097. [PubMed: 12045049]
4. Wang JJ, Rochtchina E, Lee AJ, Chia EM, Smith W, Cumming RG, et al. Ten-year incidence and progression of age-related maculopathy: the blue Mountains Eye Study. *Ophthalmology*. 2007; 114(1):92–98. [PubMed: 17198852]
5. Peeters A, Magliano DJ, Stevens J, Duncan BB, Klein R, Wong TY. Changes in abdominal obesity and age-related macular degeneration: the Atherosclerosis Risk in Communities Study. *Arch Ophthalmol*. 2008; 126(11):1554–1560. [PubMed: 19001224]
6. Seddon JM, Cote J, Davis N, Rosner B. Progression of age-related macular degeneration: association with body mass index, waist circumference, and waist-hip ratio. *Arch Ophthalmol*. 2003; 121(6):785–792. [PubMed: 12796248]
7. Edwards AO, Ritter R 3rd, Abel KJ, Manning A, Panhuysen C, Farrer LA. Complement factor H polymorphism and age-related macular degeneration. *Science*. 2005; 308(5720):421–424. [PubMed: 15761121]

8. Haines JL, Hauser MA, Schmidt S, Scott WK, Olson LM, Gallins P, et al. Complement factor H variant increases the risk of age-related macular degeneration. *Science*. 2005; 308(5720):419–421. [PubMed: 15761120]
9. Klein RJ, Zeiss C, Chew EY, Tsai JY, Sackler RS, Haynes C, et al. Complement factor H polymorphism in age-related macular degeneration. *Science*. 2005; 308(5720):385–389. [PubMed: 15761122]
10. Li M, Atmaca-Sonmez P, Othman M, Branham KE, Khanna R, Wade MS, et al. CFH haplotypes without the Y402H coding variant show strong association with susceptibility to age-related macular degeneration. *Nat Genet*. 2006; 38(9):1049–1054. [PubMed: 16936733]
11. Gold B, Merriam JE, Zernant J, Hancox LS, Taiber AJ, Gehrs K, et al. Variation in factor B (BF) and complement component 2 (C2) genes is associated with age-related macular degeneration. *Nat Genet*. 2006; 38(4):458–462. [PubMed: 16518403]
12. McKay GJ, Silvestri G, Patterson CC, Hogg RE, Chakravarthy U, Hughes AE. Further assessment of the complement component 2 and factor B region associated with age-related macular degeneration. *Invest Ophthalmol Vis Sci*. 2009; 50(2):533–539. [PubMed: 18806297]
13. Spencer KL, Hauser MA, Olson LM, Schmidt S, Scott WK, Gallins P, et al. Protective effect of complement factor B and complement component 2 variants in age-related macular degeneration. *Hum Mol Genet*. 2007; 16(16):1986–1992. [PubMed: 17576744]
14. Yates JR, Sepp T, Matharu BK, Khan JC, Thurlby DA, Shahid H, et al. Complement C3 variant and the risk of age-related macular degeneration. *N Engl J Med*. 2007; 357(6):553–561. [PubMed: 17634448]
15. Dewan A, Liu M, Hartman S, Zhang SS, Liu DT, Zhao C, et al. HTRA1 promoter polymorphism in wet age-related macular degeneration. *Science*. 2006; 314(5801):989–992. [PubMed: 17053108]
16. Jakobsondtir J, Conley YP, Weeks DE, Mah TS, Ferrell RE, Gorin MB. Susceptibility genes for age-related maculopathy on chromosome 10q26. *Am J Hum Genet*. 2005; 77(3):389–407. [PubMed: 16080115]
17. Kanda A, Chen W, Othman M, Branham KE, Brooks M, Khanna R, et al. A variant of mitochondrial protein LOC387715/ARMS2, not HTRA1, is strongly associated with age-related macular degeneration. *Proc Natl Acad Sci U S A*. 2007; 104(41):16227–16232. [PubMed: 17884985]
18. Rivera A, Fisher SA, Fritsche LG, Keilhauer CN, Lichtner P, Meitinger T, et al. Hypothetical LOC387715 is a second major susceptibility gene for age-related macular degeneration, contributing independently of complement factor H to disease risk. *Hum Mol Genet*. 2005; 14(21):3227–3236. [PubMed: 16174643]
19. Yang Z, Camp NJ, Sun H, Tong Z, Gibbs D, Cameron DJ, et al. A variant of the HTRA1 gene increases susceptibility to age-related macular degeneration. *Science*. 2006; 314(5801):992–993. [PubMed: 17053109]
20. Fritsche LG, Loenhardt T, Janssen A, Fisher SA, Rivera A, Keilhauer CN, et al. Age-related macular degeneration is associated with an unstable ARMS2 (LOC387715) mRNA. *Nat Genet*. 2008; 40(7):892–896. [PubMed: 18511946]
21. SanGiovanni JP, Arking DE, Iyengar SK, Elashoff M, Clemons TE, Reed GF, et al. Mitochondrial DNA variants of respiratory complex I that uniquely characterize haplogroup T2 are associated with increased risk of age-related macular degeneration. *PLoS ONE*. 2009; 4(5):e5508. [PubMed: 19434233]
22. Canter JA, Olson LM, Spencer K, Schnetz-Boutaud N, Anderson B, Hauser MA, et al. Mitochondrial DNA polymorphism A4917G is independently associated with age-related macular degeneration. *PLoS ONE*. 2008; 3(5):e2091. [PubMed: 18461138]
23. Mullins RF, Russell SR, Anderson DH, Hageman GS. Drusen associated with aging and age-related macular degeneration contain proteins common to extracellular deposits associated with atherosclerosis, elastosis, amyloidosis, and dense deposit disease. *FASEB J*. 2000; 14(7):835–846. [PubMed: 10783137]
24. Hageman GS, Anderson DH, Johnson LV, Hancox LS, Taiber AJ, Hardisty LI, et al. A common haplotype in the complement regulatory gene factor H (HF1/CFH) predisposes individuals to age-

- related macular degeneration. *Proc Natl Acad Sci U S A*. 2005; 102(20):7227–7232. [PubMed: 15870199]
25. Zipfel PF, Hallstrom T, Hammerschmidt S, Skerka C. The complement fitness factor H: role in human diseases and for immune escape of pathogens, like pneumococci. *Vaccine*. 2008; 26(Suppl 8):I67–I74. [PubMed: 19388168]
 26. Coffey PJ, Gias C, McDermott CJ, Lundh P, Pickering MC, Sethi C, et al. Complement factor H deficiency in aged mice causes retinal abnormalities and visual dysfunction. *Proc Natl Acad Sci U S A*. 2007; 104(42):16651–16656. [PubMed: 17921253]
 27. Dupuis J, Langenberg C, Prokopenko I, Saxena R, Soranzo N, Jackson AU, et al. New genetic loci implicated in fasting glucose homeostasis and their impact on type 2 diabetes risk. *Nat Genet*. 2006; 38(2):105–116. [PubMed: 16734137]
 28. Kathiresan S, Willer CJ, Peloso GM, Demissie S, Musunuru K, Schadt EE, et al. Common variants at 30 loci contribute to polygenic dyslipidemia. *Nat Genet*. 2009; 41(1):56–65. [PubMed: 19060906]
 29. Newton-Cheh C, Johnson T, Gateva V, Tobin MD, Bochud M, Coin L, et al. Genome-wide association study identifies eight loci associated with blood pressure. *Nat Genet*. 2009; 41(5):698–704. [PubMed: 19432157]
 30. Cupples LA, Arruda HT, Benjamin EJ, D'Agostino RB Sr, Demissie S, DeStefano AL, et al. The Framingham Heart Study 100K SNP genome-wide association study resource: overview of 17 phenotype working group reports. *BMC Med Genet*. 2007; 8(Suppl 1):S1. [PubMed: 17903291]
 31. Maller J, George S, Purcell S, Fagerness J, Altshuler D, Daly MJ, et al. Common variation in three genes, including a noncoding variant in CFH, strongly influences risk of age-related macular degeneration. *Nat Genet*. 2006; 38(9):1055–1059. [PubMed: 16936732]
 32. El-Amraoui A, Schonn JS, Kussel-Andermann P, Blanchard S, Desnos C, Henry JP, et al. MyRIP, a novel Rab effector, enables myosin VIIa recruitment to retinal melanosomes. *EMBO Rep*. 2002; 3(5):463–470. [PubMed: 11964381]
 33. Klomp AE, Teofilo K, Legacki E, Williams DS. Analysis of the linkage of MYRIP and MYO7A to melanosomes by RAB27A in retinal pigment epithelial cells. *Cell Motil Cytoskeleton*. 2007; 64(6):474–487. [PubMed: 17352418]
 34. Augustin I, Rosenmund C, Sudhof TC, Brose N. Munc13-1 is essential for fusion competence of glutamatergic synaptic vesicles. *Nature*. 1999; 400(6743):457–461. [PubMed: 10440375]
 35. Augustin I, Korte S, Rickmann M, Kretschmar HA, Sudhof TC, Herms JW, et al. The cerebellum-specific Munc13 isoform Munc13-3 regulates cerebellar synaptic transmission and motor learning in mice. *J Neurosci*. 2001; 21(1):10–17. [PubMed: 11150314]
 36. Iyengar SK, Song D, Klein BE, Klein R, Schick JH, Humphrey J, et al. Dissection of genomewide-scan data in extended families reveals a major locus and oligogenic susceptibility for age-related macular degeneration. *Am J Hum Genet*. 2004; 74(1):20–39. [PubMed: 14691731]
 37. Schraermeyer U, Heimann K. Current understanding on the role of retinal pigment epithelium and its pigmentation. *Pigment Cell Res*. 1999; 12(4):219–236. [PubMed: 10454290]
 38. Bergmann M, Schutt F, Holz FG, Kopitz J. Inhibition of the ATP-driven proton pump in RPE lysosomes by the major lipofuscin fluorophore A2-E may contribute to the pathogenesis of age-related macular degeneration. *FASEB J*. 2004; 18(3):562–564. [PubMed: 14715704]
 39. Holz FG, Schutt F, Kopitz J, Eldred GE, Kruse FE, Volcker HE, et al. Inhibition of lysosomal degradative functions in RPE cells by a retinoid component of lipofuscin. *Invest Ophthalmol Vis Sci*. 1999; 40(3):737–743. [PubMed: 10067978]
 40. Guo Y, Yao G, Lei B, Tan J. Monte Carlo model for studying the effects of melanin concentrations on retina light absorption. *J Opt Soc Am A Opt Image Sci Vis*. 2008; 25(2):304–311. [PubMed: 18246163]
 41. El-Amraoui A, Sahly I, Picaud S, Sahel J, Abitbol M, Petit C. Human Usher 1B/mouse shaker-1: the retinal phenotype discrepancy explained by the presence/absence of myosin VIIA in the photoreceptor cells. *Hum Mol Genet*. 1996; 5(8):1171–1178. [PubMed: 8842737]
 42. Weil D, Levy G, Sahly I, Levi-Acobas F, Blanchard S, El-Amraoui A, et al. Human myosin VIIA responsible for the Usher 1B syndrome: a predicted membrane-associated motor protein expressed in developing sensory epithelia. *Proc Natl Acad Sci U S A*. 1996; 93(8):3232–3237. [PubMed: 8622919]

43. Weil D, Blanchard S, Kaplan J, Guilford P, Gibson F, Walsh J, et al. Defective myosin VIIA gene responsible for Usher syndrome type 1B. *Nature*. 1995; 374(6517):60–61. [PubMed: 7870171]
44. Hasson T, Heintzelman MB, Santos-Sacchi J, Corey DP, Mooseker MS. Expression in cochlea and retina of myosin VIIa, the gene product defective in Usher syndrome type 1B. *Proc Natl Acad Sci U S A*. 1995; 92(21):9815–9819. [PubMed: 7568224]
45. Lopes VS, Ramalho JS, Owen DM, Karl MO, Strauss O, Futter CE, et al. The ternary Rab27a-Myrip-Myosin VIIa complex regulates melanosome motility in the retinal pigment epithelium. *Traffic*. 2007; 8(5):486–499. [PubMed: 17451552]
46. Kuroda TS, Fukuda M. Identification and biochemical analysis of Slac2-c/MyRIP as a Rab27A-, myosin Va/VIIa-, and actin-binding protein. *Methods Enzymol*. 2005; 403:431–444. [PubMed: 16473609]
47. Ramalho JS, Lopes VS, Tarafder AK, Seabra MC, Hume AN. Myrip uses distinct domains in the cellular activation of myosin VA and myosin VIIA in melanosome transport. *Pigment Cell Melanoma Res*. 2009; 22(4):461–473. [PubMed: 19317802]
48. Gibbs D, Kitamoto J, Williams DS. Abnormal phagocytosis by retinal pigmented epithelium that lacks myosin VIIa, the Usher syndrome 1B protein. *Proc Natl Acad Sci U S A*. 2003; 100(11):6481–6486. [PubMed: 12743369]
49. Schonthaler HB, Lampert JM, von Lintig J, Schwarz H, Geisler R, Neuhauss SC. A mutation in the silver gene leads to defects in melanosome biogenesis and alterations in the visual system in the zebrafish mutant fading vision. *Dev Biol*. 2005; 284(2):421–436. [PubMed: 16024012]
50. Schraermeyer U, Peters S, Thumann G, Kociok N, Heimann K. Melanin granules of retinal pigment epithelium are connected with the lysosomal degradation pathway. *Exp Eye Res*. 1999; 68(2):237–245. [PubMed: 10068489]
51. Warburton S, Davis WE, Southwick K, Xin H, Woolley AT, Burton GF, et al. Proteomic and phototoxic characterization of melanolipofuscin: correlation to disease and model for its origin. *Mol Vis*. 2007; 13:318–329. [PubMed: 17392682]
52. Lee SG, Lee I, Park SH, Kang C, Song K. Identification and characterization of a human cDNA homologous to yeast SKI2. *Genomics*. 1995; 25(3):660–666. [PubMed: 7759100]
53. Schmid M, Jensen TH. The exosome: a multipurpose RNA-decay machine. *Trends Biochem Sci*. 2008; 33(10):501–510. [PubMed: 18786828]
54. Bernstein KA, Granneman S, Lee AV, Manickam S, Baserga SJ. Comprehensive mutational analysis of yeast DEXD/H box RNA helicases involved in large ribosomal subunit biogenesis. *Mol Cell Biol*. 2006; 26(4):1195–1208. [PubMed: 16449635]
55. Yang Z, Qu X, Yu CY. Features of the two gene pairs RD-SKI2W and DOM3Z-RP1 located between complement component genes factor B and C4 at the MHC class III region. *Front Biosci*. 2001; 6:D927–D935. [PubMed: 11487501]
56. Chen CY, Gherzi R, Ong SE, Chan EL, Rajmakers R, Pruijn GJ, et al. AU binding proteins recruit the exosome to degrade ARE-containing mRNAs. *Cell*. 2001; 107(4):451–464. [PubMed: 11719186]
57. Wang AL, Lukas TJ, Yuan M, Du N, Tso MO, Neufeld AH. Autophagy and exosomes in the aged retinal pigment epithelium: possible relevance to drusen formation and age-related macular degeneration. *PLoS ONE*. 2009; 4(1):e4160. [PubMed: 19129916]
58. Kondo N, Honda S, Kuno SI, Negi A. Role of RDBP and SKIV2L Variants in the Major Histocompatibility Complex Class III Region in Polypoidal Choroidal Vasculopathy Etiology. *Ophthalmology*. 2009; 116(8):1502–1509. [PubMed: 19556007]
59. Fernando MM, Stevens CR, Sabeti PC, Walsh EC, McWhinnie AJ, Shah A, et al. Identification of two independent risk factors for lupus within the MHC in United Kingdom families. *PLoS Genet*. 2007; 3(11):e192. [PubMed: 17997607]
60. Edwards AO, Fridley BL, James KM, Sharma AK, Cunningham JM, Tosakulwong N. Evaluation of clustering and genotype distribution for replication in genome wide association studies: the age-related eye disease study. *PLoS One*. 2008; 3(11):e3813. [PubMed: 19043567]
61. Zhang H, Morrison MA, Dewan A, Adams S, Andreoli M, Huynh N, et al. The NEI/NCBI dbGAP database: genotypes and haplotypes that may specifically predispose to risk of neovascular age-related macular degeneration. *BMC Med Genet*. 2008; 9:51. [PubMed: 18541031]

62. Klein R, Knudtson MD, Klein BE, Wong TY, Cotch MF, Liu K, et al. Inflammation, complement factor h, and age-related macular degeneration: the Multi-ethnic Study of Atherosclerosis. *Ophthalmology*. 2008; 115(10):1742–1749. [PubMed: 18538409]
63. Tedeschi-Blok N, Buckley J, Varma R, Triche TJ, Hinton DR. Population-based study of early age-related macular degeneration: role of the complement factor H Y402H polymorphism in bilateral but not unilateral disease. *Ophthalmology*. 2007; 114(1):99–103. [PubMed: 17198853]
64. Grassi MA, Fingert JH, Scheetz TE, Roos BR, Ritch R, West SK, et al. Ethnic variation in AMD-associated complement factor H polymorphism p.Tyr402His. *Hum Mutat*. 2006; 27(9):921–925. [PubMed: 16865697]
65. Chu J, Zhou CC, Lu N, Zhang X, Dong FT. Genetic variants in three genes and smoking show strong associations with susceptibility to exudative age-related macular degeneration in a Chinese population. *Chin Med J (Engl)*. 2008; 121(24):2525–2533. [PubMed: 19187590]
66. Xu Y, Guan N, Xu J, Yang X, Ma K, Zhou H, et al. Association of CFH, LOC387715, and HTRA1 polymorphisms with exudative age-related macular degeneration in a northern Chinese population. *Mol Vis*. 2008; 14:1373–1381. [PubMed: 18682812]
67. Wang G, Spencer KL, Scott WK, Whitehead P, Court BL, Ayala-Haedo J, et al. Analysis of the indel at the ARMS2 3'UTR in age-related macular degeneration. *Hum Genet*.
68. Orlin A, Hadley D, Brown G, Brucker A, Ho A, Regillo C, et al. The Relationship Between the A69S Variant With the Indel (372_815delins54) in the ARMS2 Gene, and Its Association With Age-Related Macular Degeneration. ARVO. 2009 Abstract #1601.
69. Yang Z, Tong Z, Chen Y, Zeng J, Lu F, Sun X, et al. Genetic and functional dissection of HTRA1 and LOC387715 in age-related macular degeneration. *PLoS Genet*. 6(2):e1000836. [PubMed: 20140183]
70. Fei H, Grygoruk A, Brooks ES, Chen A, Krantz DE. Trafficking of vesicular neurotransmitter transporters. *Traffic*. 2008; 9(9):1425–1436. [PubMed: 18507811]
71. Newell-Litwa K, Seong E, Burmeister M, Faundez V. Neuronal and non-neuronal functions of the AP-3 sorting machinery. *J Cell Sci*. 2007; 120(Pt 4):531–541. [PubMed: 17287392]
72. Mailman MD, Feolo M, Jin Y, Kimura M, Tryka K, Bagoutdinov R, et al. The NCBI dbGaP database of genotypes and phenotypes. *Nat Genet*. 2007; 39(10):1181–1186. [PubMed: 17898773]
73. Age Related Eye Disease Study Group. Risk factors associated with age-related macular degeneration. A case-control study in the age-related eye disease study: Age-Related Eye Disease Study Report Number 3. *Ophthalmology*. 2000; 107(12):2224–2232. [PubMed: 11097601]
74. Ferris FL, Davis MD, Clemons TE, Lee LY, Chew EY, Lindblad AS, et al. A simplified severity scale for age-related macular degeneration: AREDS Report No. 18. *Arch Ophthalmol*. 2005; 123(11):1570–1574. [PubMed: 16286620]
75. Klein R, Klein BE, Jensen SC, Meuer SM. The five-year incidence and progression of age-related maculopathy: the Beaver Dam Eye Study. *Ophthalmology*. 1997; 104(1):7–21. [PubMed: 9022098]
76. Klein R, Klein BE, Linton KL. Prevalence of age-related maculopathy. The Beaver Dam Eye Study. *Ophthalmology*. 1992; 99(6):933–943. [PubMed: 1630784]
77. S.A.G.E. Statistical Analysis for Genetic Epidemiology. 2007 <http://genepi.cwru.edu>.
78. Marchini J, Howie B, Myers S, McVean G, Donnelly P. A new multipoint method for genome-wide association studies by imputation of genotypes. *Nat Genet*. 2007; 39(7):906–913. [PubMed: 17572673]
79. Devlin B, Roeder K. Genomic control for association studies. *Biometrics*. 1999; 55(4):997–1004. [PubMed: 11315092]
80. Purcell S. PLINK. 2008 <http://pngu.mgh.harvard.edu/purcell/plink>.
81. Purcell S, Neale B, Todd-Brown K, Thomas L, Ferreira MA, Bender D, et al. PLINK: A Tool Set for Whole-Genome Association and Population-Based Linkage Analyses. *Am J Hum Genet*. 2007; 81(3):559–575. [PubMed: 17701901]
82. Li, Y.; Abecasis, G. Markov Chain Haplotyping. MACH; 2009.
83. Stephens M, Smith NJ, Donnelly P. A new statistical method for haplotype reconstruction from population data. *Am J Hum Genet*. 2001; 68(4):978–989. [PubMed: 11254454]

84. Stephens M, Scheet P. Accounting for decay of linkage disequilibrium in haplotype inference and missing-data imputation. *Am J Hum Genet.* 2005; 76(3):449–462. [PubMed: 15700229]

Author Manuscript

Author Manuscript

Author Manuscript

Author Manuscript

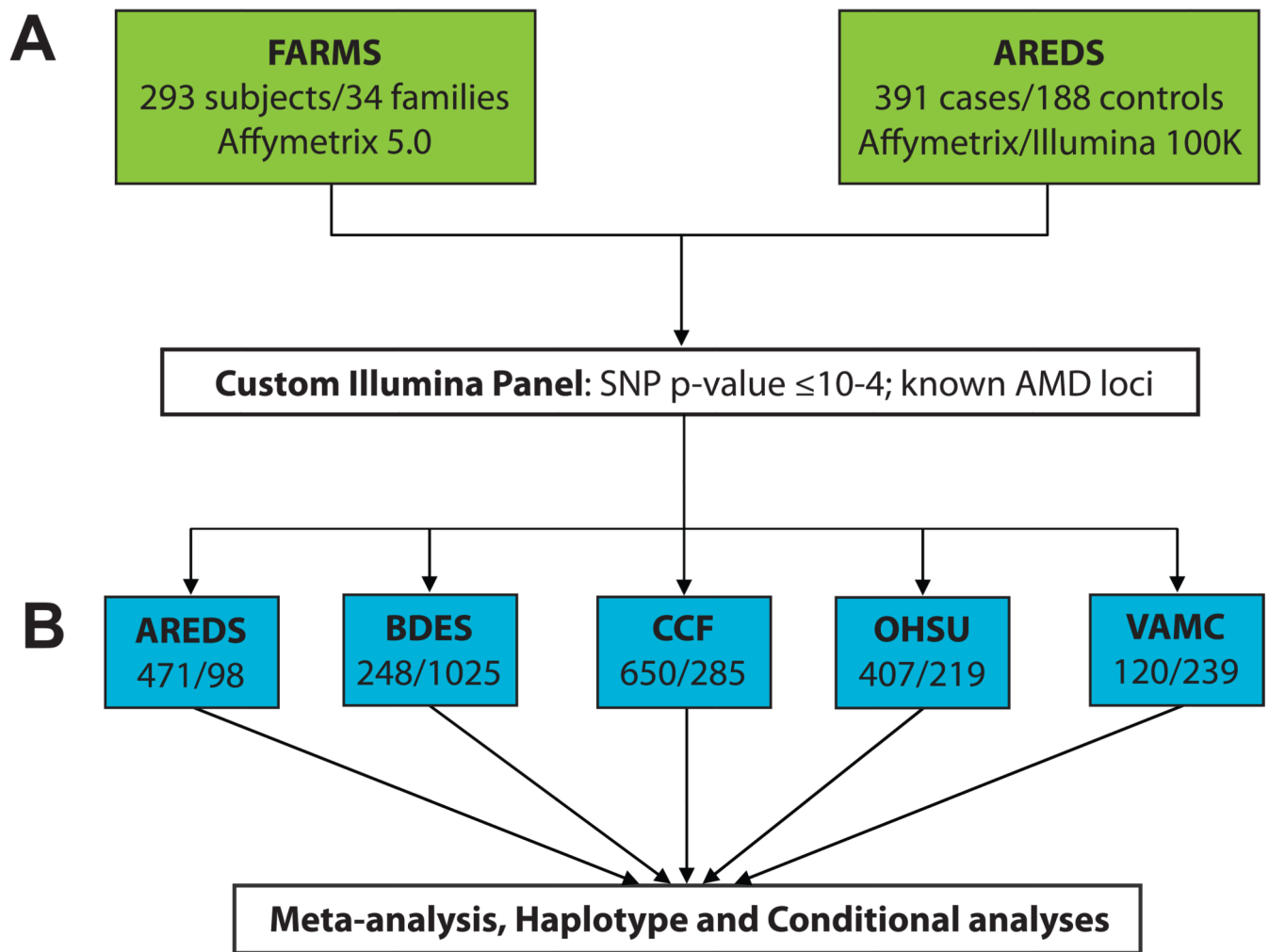


Figure 1.

Overall study workflow. The study consisted of a two-phase design. A. The initial discovery phase consisted of genome-wide association testing in two cohorts (FARMS, a family-based analysis, and AREDS, a case/control analysis). B. The second phase tested the most significant findings from the discovery cohorts and additional markers at previously identified AMD loci in five additional case/control cohorts. Numbers beneath cohort designations indicate the number of cases/controls included in the replication analysis.

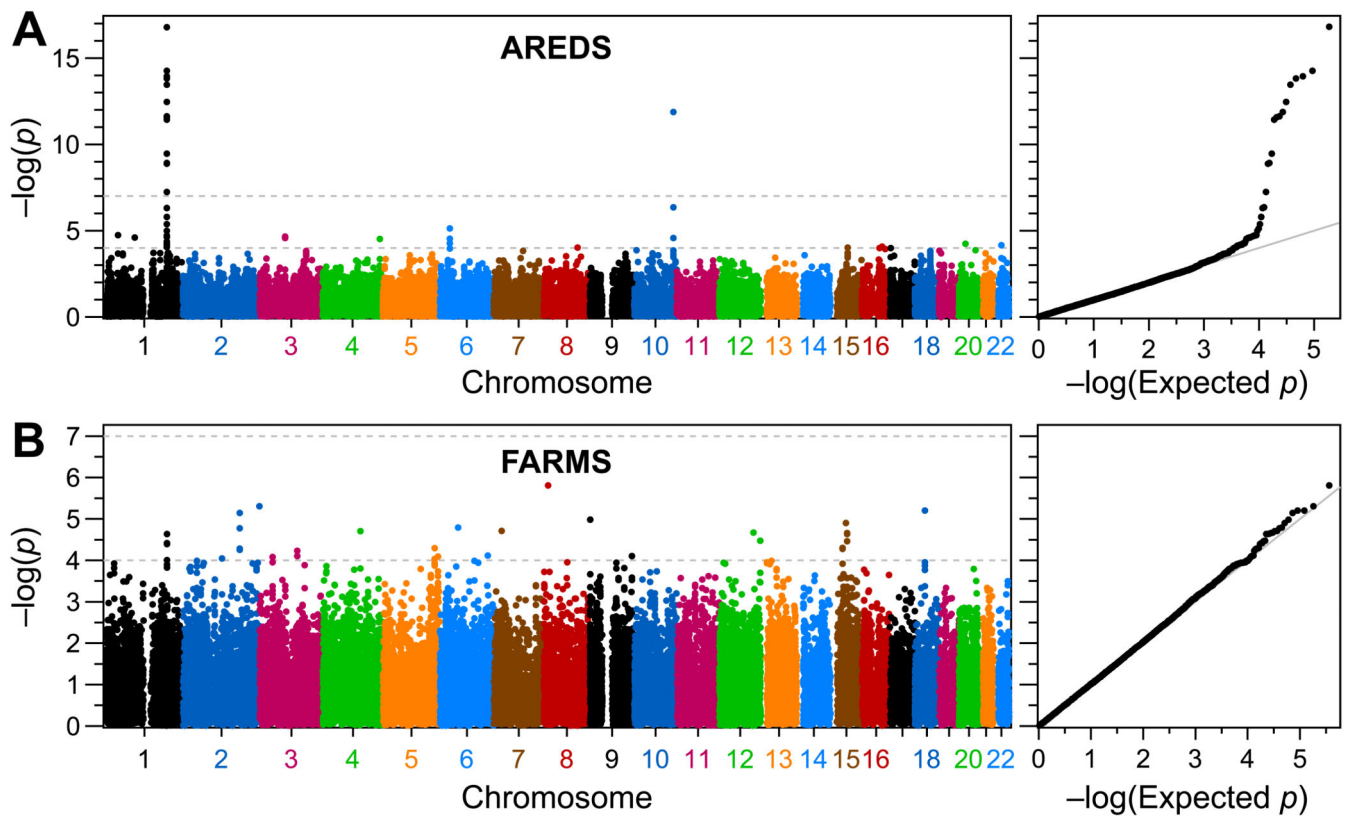


Figure 2. Results from GWAS in AREDS and FARMS. A. Manhattan plot of results from association testing in the AREDS cohort and QQ plot of observed vs. expected p-values. B. Manhattan and QQ plot for FARMS association results.

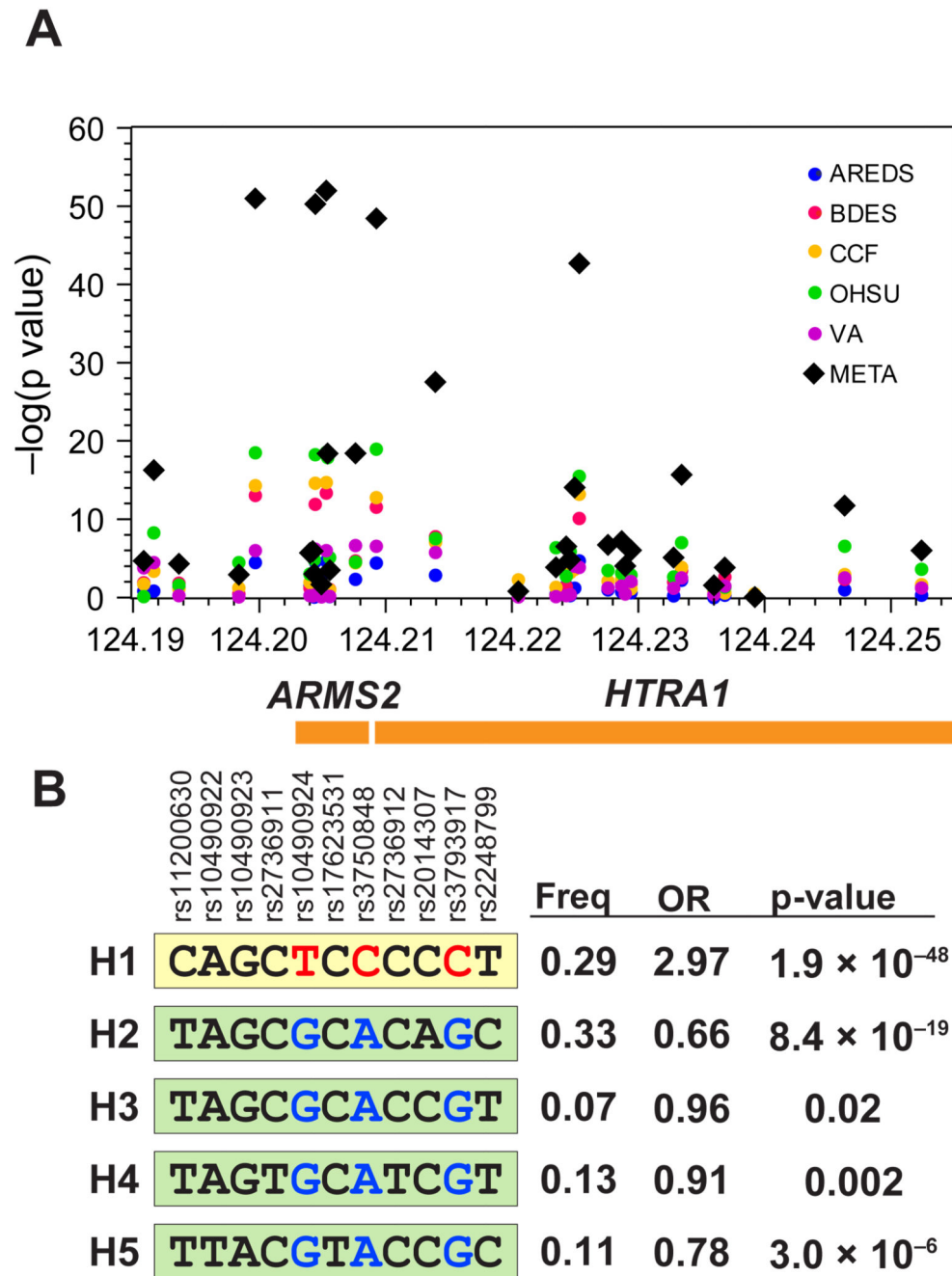


Figure 3. ARMS2 replication association results. A. Results of single SNP association testing at the ARMS2/HTRA1 locus. Results for each individual replication cohort and the results from meta-analysis are displayed. B. Results from haplotype association testing at this locus. Red/blue colored SNPs indicate the risk/protective alleles at three SNPs that were also identified in Fritsche *et al*²⁰ as defining a risk haplotype bearing an indel polymorphism at ARMS2.

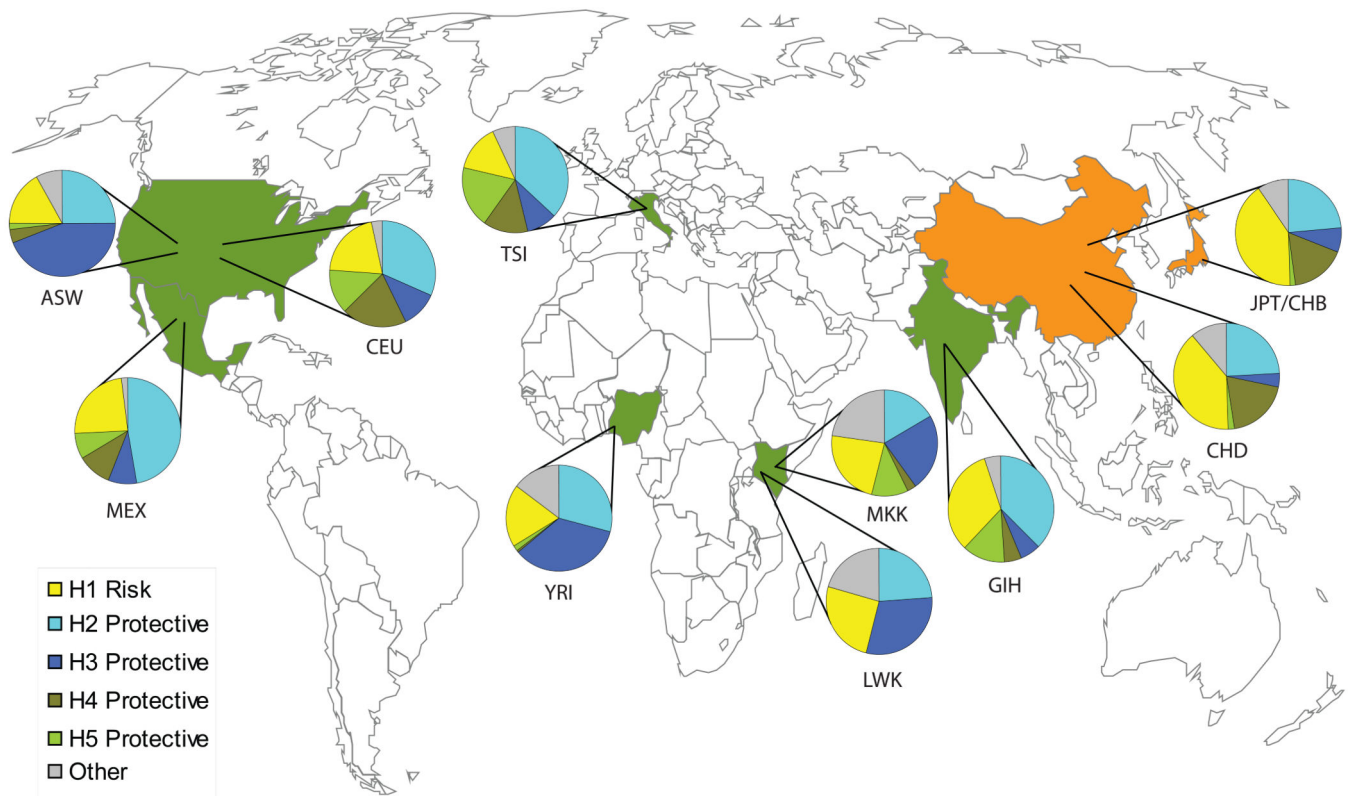
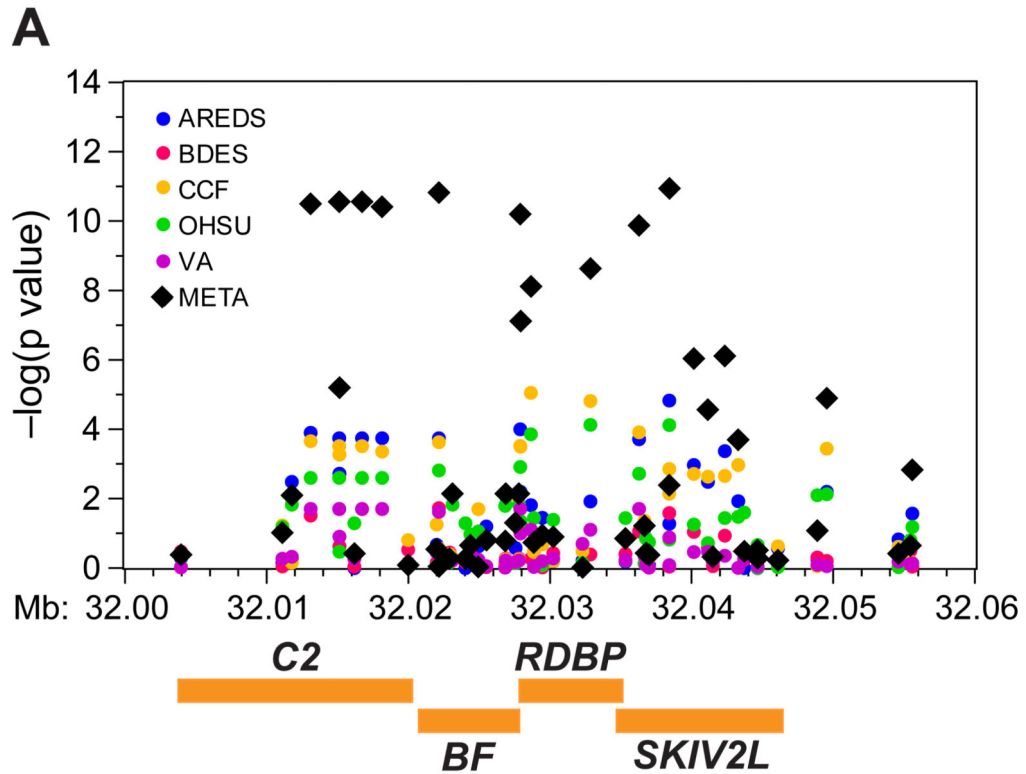


Figure 4. ARMS2 haplotype frequencies in HapMap populations. Frequencies of the risk haplotype and four protective haplotypes in the original and HapMap3 populations are shown. ASW-African ancestry in Southwest USA; CEU-Utah residents with Northern and Western European ancestry; CHB-Han Chinese in Beijing, China; CHD-Chinese in metropolitan Denver, USA; GIH-Gujarati Indians in Houston, TX; JPT-Japanese in Tokyo, Japan; LWK-Luhya in Webuye, Kenya; MEX-Mexican ancestry in Los Angeles, California; MKK-Maasai in Kinyawa, Kenya; TSI-Toscani in Italy; YRI-Yoruba in Ibadan, Nigeria.



B

	rs1042663 rs550605* rs653414 rs497239* rs609061* rs641153* rs522162* rs760070 rs550513* rs403569* rs438999 rs429608 rs406936	Freq	OR	p-value
H1	GTCTGGTTCGAGG	0.82	1.36	1.9×10^{-5}
H2	GTCTGGTTCGAAG	0.05	0.72	0.01
H3	ACTCAACCTAGAA	0.04	0.32	1.2×10^{-9}
H4	ACTCAACCCGGAA	0.02	0.52	0.005
H5	GTCTGGTTCGAGA	0.04	1.04	0.79

Figure 5. SKIV2L replication association results. A. Results of single SNP association testing at the C2/SKIV2L region in the five replication cohorts. The meta-analysis findings are also displayed. B. Risk modifying haplotypes at the chromosome 6 locus. The risk and protective alleles of rs429608 are indicated in red and blue respectively.

Table 1

Significant findings in discovery and replication cohorts.

SNP	Description	CHR	Position	MA	Meta-Analysis			AREDS		FARMS		Fisher's	
					OR	p	Q	OR	p	β	p	p	
Known AMD Loci													
rs1061170	CFH, Y402H	1	194,925,860	C	2.30	2.6×10^{-42}	12.7	2.70	4.8×10^{-12}	0.58^*	3.9×10^{-5}	4.0×10^{-42}	
rs1329428	CFH, intron	1	194,969,433	T	0.36	1.9×10^{-52}	20.2	0.30*	2.1×10^{-15}	-0.48^*	0.002	3.2×10^{-64}	
rs10490924	ARMS2, A69S	10	124,204,438	T	2.75	5.5×10^{-51}	8.9	3.38	2.8×10^{-15}	0.45	0.0017	1.2×10^{-60}	
rs3750848	ARMS2, intron	10	124,205,305	G	2.76	1.1×10^{-52}	8.5	3.20*	9.8×10^{-13}	0.45	0.0017	8.1×10^{-60}	
rs3793917	HTRA1, promoter	10	124,209,265	G	2.67	3.7×10^{-49}	11.2	3.18*	1.2×10^{-12}	0.46^*	0.0016	4.2×10^{-57}	
rs641153	BF, R32Q	6	32,022,159	A	0.46*	1.5×10^{-11}	2.6	0.38*	5.0×10^{-5}	-0.85^*	0.0027	6.8×10^{-14}	
rs429608	SKI2L, intron	6	32,038,441	A	0.54	1.1×10^{-11}	5.6	0.41	7.2×10^{-6}	-0.81^*	0.0058	5.3×10^{-15}	
rs2230199	C3, R102G	19	6,669,387	C	1.44	1.6×10^{-7}	5.0	1.86	7.5×10^{-5}	0.21^{**}	0.19	1.4×10^{-8}	
Novel AMD Locus													
rs2679798	MYRIP, intron	3	40,226,286	G	0.86	0.007	3.3	1.05*	0.73	-0.50^*	0.00037	2.9×10^{-4}	
rs11129874	MYRIP, 3'	3	40,301,169	C	0.88	0.03	2.0	0.94*	0.63	-0.54	8.3×10^{-5}	0.0014	
rs1344189	MYRIP, intron	3	40,224,248	C	0.86	0.01	2.8	1.04*	0.76	-0.50^*	0.00023	3.4×10^{-4}	

Data from the five replication cohorts was combined via meta-analysis and is presented here in this summarized form. Fisher's p-values combined results from both discovery cohorts and the five replication cohorts. MA-minor allele; OR-odds ratio; Q-Q heterogeneity statistic; Q-Q regression coefficient;

* Indicates imputed SNP;

** Genotyped using a TaqMan assay